Available online at www.sciencedirect.com
ScienceDirect
C. R. Physique 10 (2009) 252–267
COMPTES RENDUS PHYSIQUE

Carbon nanotube electronics / Électronique à nanotubes de carbone

Superconducting properties of carbon nanotubes

M. Ferrier, A. Kasumov, R. Deblock, S. Guéron, H. Bouchiat *

Univ. Paris-Sud, CNRS, UMR 8502, 91405 Orsay cedex, France

Received 17 March 2009; accepted 22 April 2009

Available online 27 June 2009

Abstract

Metallic single wall carbon nanotubes have attracted much interest as 1D quantum wires combining a low carrier density and a high mobility. It was believed for a long time that low temperature transport was exclusively dominated by the existence of unscreened Coulomb interactions leading to an insulating behavior at low temperature. However experiments have also shown evidence of superconductivity in carbon nanotubes. We distinguish two fundamentally different physical situations. When carbon nanotubes are connected to superconducting electrodes, they exhibit proximity induced superconductivity with supercurrents which strongly depend on the transmission of the electrodes. On the other hand intrinsic superconductivity was also observed in suspended ropes of carbon nanotubes and recently in doped individual tubes. These experiments indicate the presence of attractive interactions in carbon nanotubes which overcome Coulomb repulsion at low temperature, and enables investigation of superconductivity in a 1D limit never explored before. ***To cite this article: M. Ferrier et al., C. R. Physique 10 (2009).***

Résumé

Propriétés supraconductrices des nanotubes de carbone. Les nanotubes de carbone monofeuillets, en combinant une faible densité électronique et une forte mobilité, ont attiré un intérêt considérable en tant que système modèle pour l'étude du transport quantique à une dimension. Dans ce type de système le transport à basse température était prédit être dominé par l'existence d'interactions coulombiennes non écrantées donnant lieu à un comportement isolant à basse température. Mais les expériences montrent, quant à elles, l'existence de supraconductivité dans les nanotubes de carbone. Il est important de distinguer deux situations physiques bien différentes. Dans la première, lorsque ils sont connectés à des électrodes supraconductrices, les nanotubes de carbone deviennent supraconducteurs par effet de proximité avec des supercourants dont l'intensité dépend très fortement de la transmission des électrodes. Dans la seconde, lorqu'ils sont connectés à des contacts normaux, il a été aussi possible d'observer de la supraconductivité intrinsèque dans des faisceaux suspendus de nanotube de carbone et plus récemment dans des nanotubes individuels dopés. Ces expériences montrent l'existence d'interactions attractives qui dominent la répulsion coulombienne à basse température, ce qui permet une exploration de la supraconductivité dans une limite unidimensionnelle jamais encore atteinte. ***Pour citer cet article : M. Ferrier et al., C. R. Physique 10 (2009).***

Keywords: Carbon nanotubes; Phase coherent transport; Proximity induced superconductivity; Josephson effect; Intrinsic superconductivity

Mots-clés : Nanotubes de carbone ; Transport quantique cohérent ; Supraconductivité de proximité ; Effet Josephson ; Supraconductivité intrinsèque

* Corresponding author.
E-mail address: bouchiat@lps.u-psud.fr (H. Bouchiat).

1631-0705/$ – see front matter
doi:10.1016/j.crhy.2009.04.004

1. Introduction

Single wall carbon nanotubes are constituted by a single graphene sheet wrapped into a cylinder. The Fermi surface of graphene is very particular, it is reduced to six discrete points at the corners of the first Brillouin zone [1]. As a result, depending on their diameter and their helicity which determine the boundary conditions of the electronic wave functions around the tube, SWNT can be either semiconducting or metallic [2,3]. When metallic they have only two conducting channels [2]. The minimum resistance of a single wall nanotube in good contact with normal electrodes is thus $R_Q/2$ where $R_Q = h/(2e^2) = 12.9\ \mathrm{k}\Omega$ is the resistance quantum.

It has been shown that these two conduction modes of carbon nanotubes are only very weakly coupled by electron interactions. SWNT are thus expected to exhibit electronic properties similar to systems presenting 1D conducting ladders with very small transverse coupling. In such 1D systems electron–electron interactions have been shown to determine the low temperature properties, with a non-Fermi liquid behavior characteristic of a Luttinger liquid state (LL) [4,5] with collective low energy plasmon-like excitations giving rise to anomalies in the single particle density of states. Proof of the validity of the LL description with repulsive interactions in SWNT was given by the measurement of a resistance diverging as a power law with temperature down to 10 K [6] with an exponent depending on whether contacts are taken on the end or in the bulk of the tube. This power law behavior would lead to an insulating state at very low temperature.

However, in these measurements the nanotubes are separated from measuring leads by tunnel junctions. The low temperature transport corresponding to $k_B T < E_C$ is dominated by Coulomb blockade [7], where $E_C = e^2/C$ of the order of 10 K is the charging energy of the nanotube of capacitance $C = \epsilon L/\ln(L/R)$ (L and R being respectively the length and radius of the nanotube and ϵ the effective dielectric constant of its surrounding medium). In contrast it is also possible to investigate transport through carbon nanotubes in good contacts with metallic and possibly superconducting electrodes.

Individual metallic tubes with a room temperature resistance between 10 kΩ and 40 kΩ, were obtained either using the nanosoldering technique developed by A. Kasumov [8] or by burying the tube ends over a large distance under metallic electrodes fabricated with electron beam lithography [9,10]. The resistance increases only slightly at low temperatures (typically a 20% resistance increase between RT and 1 K). The current versus voltage (I–V) curves also exhibit logarithmic non-linearities at low temperature, in stark contrast with the temperature and bias dependences of tubes with tunnel contacts. It is not surprising that in addition to the intrinsic conducting properties of tubes (interactions, band structure, disorder), the way they are contacted should determine the temperature dependence of the resistance. Extrapolating the results obtained on Luttinger liquids between normal reservoirs [11], the resistance of a ballistic tube on perfect contacts is expected to be insensitive to interactions and to be given by $R_Q/2 = 6.5\ \mathrm{k}\Omega$ at all temperatures, as for an ideal two channel conductor. The intermediate conduction regime is also particularly interesting with the formation, in case of an odd number of electrons on the nanotube, of a strongly correlated Kondo resonant state where the magnetic moment of the highest occupied level is screened by the spins of the electrons in the contacts [12]. Moreover, when the carbon nanotubes are in good contact with superconducting electrodes, it is possible to induce superconductivity and observe supercurrents, as was first investigated in ungated suspended devices [13,14] and then explored in gated devices with evidence of a strong modulation of subgap conductance, depending on the transmission.

More surprising, *intrinsic* superconductivity was also observed in suspended ropes of carbon nanotubes and recently in doped individual tubes. These experiments indicate the presence of attractive interactions in carbon nanotubes which overcome Coulomb repulsion at low temperature.

The article is organised as follows:

– The next section is devoted to proximity induced superconductivity focusing mostly on experiments in ungated suspended carbon nanotubes performed in our group which also offer the possibility of the investigation of transverse vibration modes. We also discuss more recent experiments on gated tubes (performed by several groups including ours) which lead to tunable Josephson junctions.

– The third section is devoted to intrinsic superconducting fluctuations observed by our group at sub Kelvin temperatures in suspended ropes of carbon nanotubes. We discuss the various parameters which influence this superconductivity like the invasive character of the normal contacts, the number of tubes and disorder within a rope, and finally the suspended character of the tubes. Magnetisation experiments on similar samples reveal a small but detectable Meissner effect, difficult to observe because of residual catalytical magnetic particles in the tubes. We finally

discuss recent experiments performed by other groups showing evidence of superconducting fluctuations at much larger temperature, above 10 K, in doped carbon nanotubes.

2. Proximity induced superconductivity in carbon nanotubes as a probe of phase coherent transport

Several transport experiments were performed on individual carbon nanotubes (SWNT) connected to superconducting electrodes. These experiments probe not only the conduction of SWNT but also the coherent nature of the transport from the observation proximity induced superconductivity below the superconducting transition temperature of the electrodes. A normal metal in good contact with macroscopic superconducting leads is in the proximity effect regime: superconducting correlations enter the normal metal over a characteristic length L_N which is the smallest of either the phase coherence length in the normal metal L_ϕ or the thermal length L_T. Both lengths, of the order of a few μm, can be much greater than the superconducting coherence length ξ of the superconducting contacts. This effect was extensively investigated in mesoscopic wires made of noble metals [15–17] connected to massive superconducting electrodes. These so called SNS junctions exhibit a Josephson effect like tunnel junctions, i.e. a supercurrent at zero bias. The maximum low temperature value of the supercurrent (critical current) in such SNS junctions of normal state resistance R_N is related to the superconducting gap Δ by: $\pi\Delta/eR_N$ in the short junction limit $L \ll \xi$ [18], and $\alpha E_c/eR_N$, with α a numerical factor of the order of 10, in the limit of long junctions $L \gg \xi$ where $E_c = \hbar/\tau_D$ and τ_D is the typical traversal time of charge carriers through the junction [16]. Probing the proximity effect in a normal wire connected to superconducting electrodes and in particular the existence of a Josephson current constitutes a powerful tool for the investigation of phase coherent transport through this normal wire.

2.1. Supercurrents in ungated suspended SWNT

Proximity induced superconductivity was first observed in suspended carbon nanotubes mounted on Ta/Au electrodes [13] which are a bilayer (5 nm Ta, 100 nm Au) with a transition temperature of the order of 0.4 K. This value is strongly reduced compared to the transition temperature of bulk tantalum (4 K) due to the large thickness of gold relative to tantalum. Tubes were soldered with a laser pulse on low resistive metallic contacts across a slit etched in a silicon nitride membrane. This technique enables both the realisation of contacts with a transmission probability of carriers between the nanotube and the electrodes close to unity, and a good characterisation of the samples by transmission electron microscopy. The temperature dependence of the low current resistance exhibits a broad transition around the superconducting transition temperature of the contacts and becomes zero at lower temperature as seen on Fig. 1. The transition is shifted to lower temperature when a magnetic field is applied in the plane of the contacts and perpendicular to the tube axis. Above 2 Tesla all signatures of superconductivity disappear: the resistance becomes field independent and slightly increases when the temperature is lowered below 0.2 K. The critical field, can be extracted as the inflection point of the magnetoresistance depicted in Fig. 1 (left); its value of the order of 1 Tesla for all samples is surprisingly high and is ten times larger than the measured critical field of the contact (0.1 T). It is possible that these high values of critical field are due to local modifications of the bilayer Ta/Au film in the contact region due to the laser pulse, in particular the melted upper gold film is probably much thinner than the original one. It is, however, important to note that the critical fields are nearly the same for the various samples measured and all vary linearly with temperature down to T_c.

The most striking signature of proximity induced superconductivity, is the existence of Josephson supercurrents through the samples at low temperature as shown in Fig. 1 (right). The transition between the superconducting state (zero voltage drop through the sample) and the dissipative (resistive) state is quite abrupt and displays hysteresis. It is characterised by a critical current $i_c = 0.14$ μA near zero temperature. The value of the product $R_N i_c$ at $T = 0$, for the 3 samples depicted in Fig. 1 (left), varies between 1.6 and 3.5 mV, it is of the order but significantly larger than the expected value of the order of the gap of pure tantalum $\Delta_{\mathrm{Ta}} = 0.7$ mV in the short junction limit.

Observation of a strong proximity effect indicates that phase coherent transport takes place in carbon nanotubes on the micron scale. However, the surprisingly high values of critical currents measured cannot be described by the theory of *SNS* junctions where the normal part *N* is a LL with repulsive interactions [19,20].

Our data could, on the other hand, be explained by the existence of superconducting fluctuations intrinsic to SWNT [21,22]. For an infinite nanotube, because of its 1D character, these fluctuations are not expected to give rise to a superconducting state at finite temperature. However, the superconducting state could be stabilised by the macroscopic

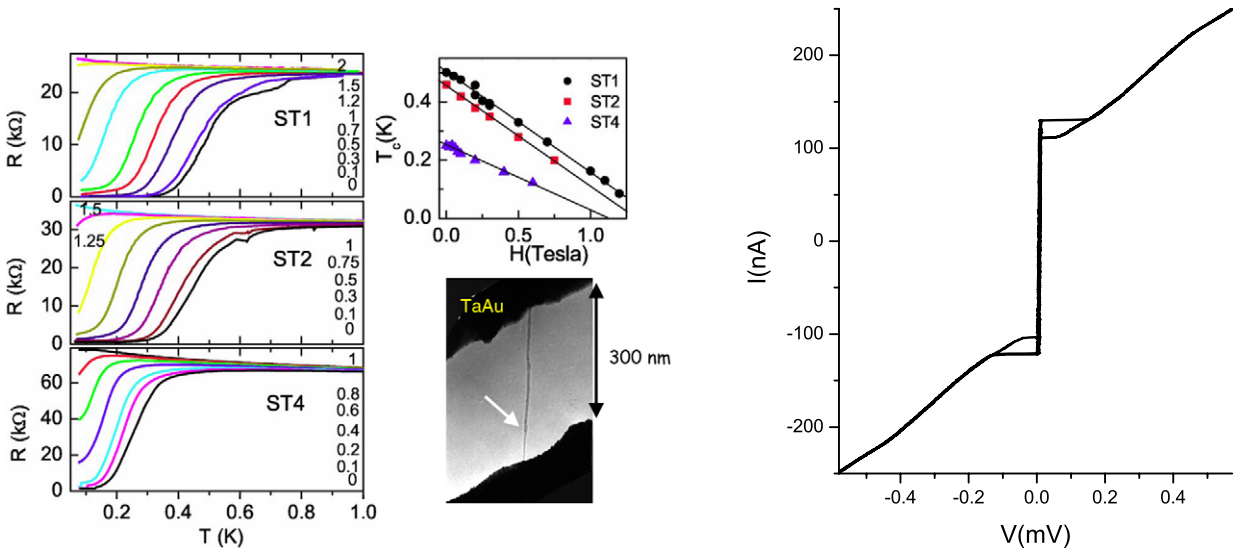

Fig. 1. Left: Temperature dependence of the resistance of 3 different single tubes ST1, 2, 4 mounted on TaAu measured for different values of the magnetic field perpendicular to the tube axis in the plane of the contacts. Bottom insert: Transmission electronic microscopy picture of the nanotube ST1 suspended between the two TaAu contacts. Top insert: Field dependence of the transition temperature (defined as the inflection point of $R(T)$). Right: Typical $I(V)$ characteristics for the suspended individual SWNT ST1 measured at 100 mK.

superconductivity of the contacts. In such a situation, it is conceivable to expect the supercurrent to be enhanced compared to its value in a conventional SNS junction and to be equal to the critical current of a superconducting filament which reads $i_c = (4e^2/h)\Delta_t$ determined by the value of the superconducting pairing amplitude Δ_t inside the wire and independent of the normal state resistance of the nanotube (in the limit where the mean free path is larger than the superconducting coherence length). We see in the next section that the observation of intrinsic superconductivity in suspended ropes of SWNT corroborates this scenario.

2.2. *Superconducting nano-electromechanical resonators based on suspended carbon nanotubes*

We show in the following that it is possible to take advantage of the extreme sensitivity of proximity induced superconductivity to dephasing events in the nanotubes and detect their transverse low frequency vibrational modes (bending modes) from transport measurements. The experiment consists in exciting vibrations on the tubes by applying a radio-frequency (rf) electromagnetic field via a macroscopic antenna. The mechanism of excitation of vibrations is explained by the presence of electrostatic charges on the tube and the Coulomb force produced by the rf electric field on these charges. The existence of charge depletion in a carbon nanotube in close contact with a noble metal such as Au or Pt has been shown to arise from the difference of electronic work functions between the SWNT and the metal [24]. The resulting uncompensated charges on a SWNT is estimated to be of the order of $q = 100e$ where e is the electron charge. If these charges are not uniformly distributed on the tube, the excitation of harmonics is favored compared to the fundamental. A similar mechanism for the excitation of mechanical resonances has been demonstrated in cantilevered multiwall nanotubes under an electron microscope [23]. When the tubes are superconducting, the mechanical vibrations induce a loss of phase coherence which is detected via a reduction of the critical current and the onset of finite resistance at large enough rf power excitation and can be simply detected via a transport experiment as shown on Fig. 2. The experimentally observed resonance frequencies are approximately multiples of 300 MHz which is the value expected for the transverse vibrations of a slightly stretched rope [25]. The fundamental frequency is, however, not observed. This absence may have an intrinsic origin (for instance the non-homogeneity of the strain along this long rope, leading to weak coupling of the fundamental mode to an homogeneous excitation), or may be simply due to the particularly small coupling to the antenna in this frequency range.

The mechanical origin of the resonances has been confirmed by the shift to lower frequencies caused by deposition of nitrogen molecules on the nanotubes. The quality factors of these resonances were found to be of the order of 1000

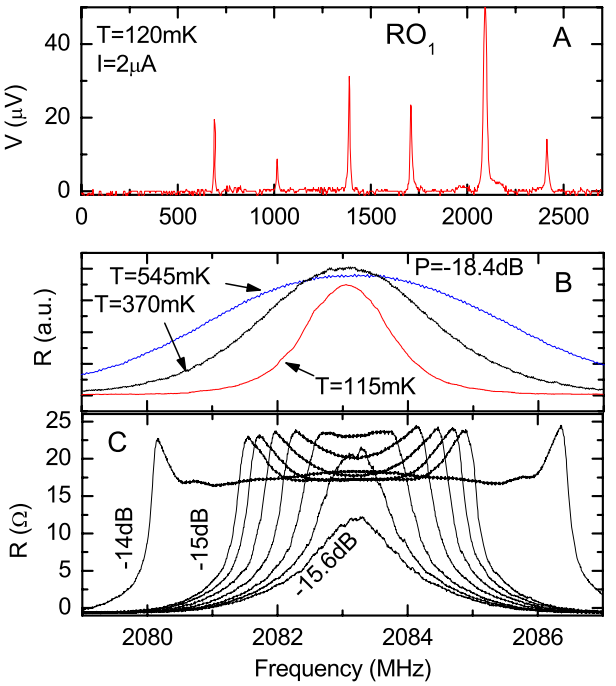

Fig. 2. A. Effect of a rf electromagnetic radiation on the dc voltage across a 1.6 μm long suspended rope of carbon nanotubes connected to superconducting electrodes when it is run through by a dc current below the critical current. B. Evolution of the resonance line shapes of the 6th harmonics with the temperature of the contacts. C. Resistance of the rope versus frequency near the 6th harmonics, at 110 mK and for different applied rf powers.

at 1 K and to increase approximatively as $1/T$ at low temperature. We have also observed non-linear effects at high RF excitation power which have not yet received clear explanations [25].

Since these preliminary experiments, mechanical resonances of carbon nanotubes have been explored in various more sophisticated experimental setups [26], but it is interesting to note that the high quality factor values we have observed probably due to the superconducting contacts were not reproduced. Superconducting nano-electromagnetic resonators have also been recently investigated theoretically [27] in the interesting regime where the Josephson frequency coincides with eigen mechanical modes in the system and deserve further experimental studies.

2.3. Tunable supercurrents in gated carbon nanotubes

Proximity induced superconductivity was also explored in devices in which the number of electrons in the nanotube can be adjusted with a gate voltage. Evidence was shown of a strong modulation of conductance at bias voltages lower than the superconducting gap, but in most cases no supercurrent was observed [28–30]. More recently, tunable supercurrents could be detected in the resonant tunneling conduction regime, where the transmission of the contacts approaches unity [31]. In this regime, the discrete spectrum of the nanotube is still preserved and the maximum value of supercurrent is observed when the Fermi energy of the electrodes is at resonance with "the-electron-in-a-box" states of the nanotube.

A superconducting quantum interference device was also fabricated with carbon nanotubes as Josephson junctions: Supercurrent π phase shifts occurred when the number of electrons in the nanotube dot was changed from even to odd [32] corresponding to the transition from a singlet (non-magnetic) to a doublet magnetic state of the dot. Sharp discontinuities in the critical current at this $0-\pi$ transition in relation with the even-odd occupation number of the nanotube quantum dot were also observed in single nanotube junction devices [33]. It was pointed out in the SQUID experiment [32] that a Josephson current can be observed in the Kondo regime, when the Kondo temperature is large compared to the superconducting gap, confirming theoretical predictions [34–39] and previous experiments [29,40] with no determination of supercurrents though, indicating that Kondo effect and proximity induced superconductivity

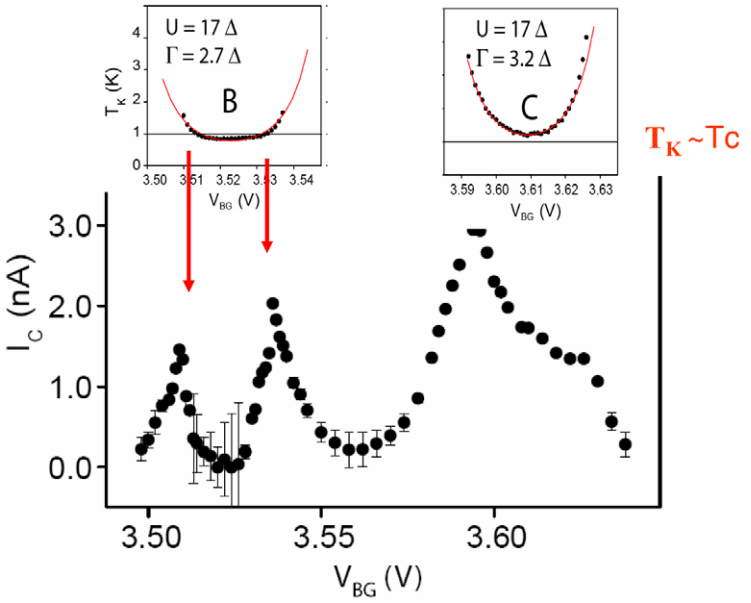

Fig. 3. Lower graph: Gate voltage dependence of the critical current measured on two successive Kondo ridges in relation with the Kondo temperature shown on the two upper insets. A sharp transition of the critical current is observed when the Kondo temperature becomes smaller than the superconducting temperature transition of the contacts (ridge B). This transition does not exist when $T_K > T_C$ along the whole Kondo ridge (ridge C) [41].

can cooperate in favoring the coherent transfer of Cooper pairs through the nanotube, provided that Kondo correlations are strong enough with $T_K > \Delta$. We have recently investigated this competition between Josephson and Kondo physics by monitoring on the same device the bias dependence of the differential conductance in the normal state and the Josephson current in the superconducting state as a function of the gate voltage [41]. A supercurrent is observed (for an odd number of electrons on the nanotube) when both energy level spacing and Kondo temperature are sufficiently high compared to the superconducting gap Δ and when the asymmetry of the transmission of the electrodes is not too large. This is understood considering that the formation of a coherent, non-magnetic, resonant Kondo singlet state on the tube prior to the onset of the BCS superconducting order, favors the transmission of Cooper pairs through the island. The induced superconducting BCS gap is only a minor perturbation in the broad Kondo resonance of width T_K. On the other hand, when the Kondo temperature is smaller than the superconducting gap, the magnetic spin remains unscreened at all temperatures leading to a sign reversal of the Josephson current phase relation (π-junction) with a very low transmission of Cooper pairs.

We have also explored [41] the intermediate regime where the Kondo temperature can be tuned with the gate voltage via the position of the energy levels with respect to the Fermi energy, from a value slightly below the superconducting gap at half filling to a value $T_K(\epsilon)$ larger than Δ. A sharp increase of the supercurrent is then observed, which is related to the transition from a magnetic to a non-magnetic state of the nanotube island as shown on Fig. 3. These results are in good agreement with functional renormalisation group (FRG) calculations for the single impurity Anderson model [39] and illustrate the extreme sensitivity of proximity induced superconductivity as a probe of magnetism at the single molecule level.

It is important to note that the values of supercurrent measured in all these experiments on gated tubes do not exceed a few nano-Amperes and are at least one order of magnitude below the theoretically expected values and the values obtained in our experiments on suspended tubes discussed above. It has been argued that uncontrolled dissipative electromagnetic environments could be responsible for this strong supercurrent reduction. It is also possible that the presence in all these experiments of a strongly doped underlying Si substrate (used as a backgate) covered by an oxide layer contributes to electromagnetic noise at high frequency. In the case of suspended nanotubes, however, we will see in the following that their suspended character seems to favor intrinsic superconducting fluctuations on normal contacts which could explain an enhancement of supercurrents in the proximity induced superconductivity regime.

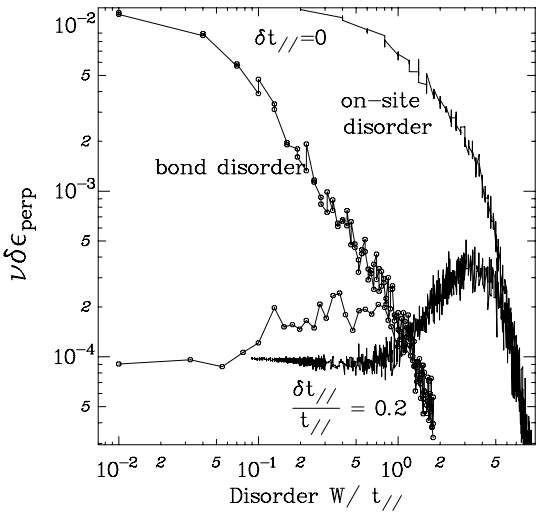

Fig. 4. Transverse delocalisation by disorder: Evolution of $\delta\epsilon_{\text{perp}}$ with the amplitude of disorder for 10 coupled chains of 100 sites, W corresponds either to on site disorder (black dots), either to bond disorder (open circles). The situation of identical values of $t_{\|}$ on all chains, corresponding to $\delta t_{\|} = 0$, upper curves, exhibits expected disorder induced localisation, whereas the situation with different values of t_n where $\delta t_{\|}/t_{\|} = 0.2$ shows a regime of disorder induced transverse delocalisation. The transverse hopping energy is chosen to be $t_{\perp} = 0.06 t_{\|}$. ν is the density of states (inverse nearest level spacing) [45].

3. Intrinsic superconductivity

3.1. Normal state transport in ropes of SWNT

A rope of single wall carbon nanotubes (SWNT) is made of ordered parallel tubes with different helicities, but with a narrow distribution of diameters [2,42]. The center of the tubes form a triangular lattice so that there is for each metallic tube in a rope on average two neighboring tubes which are also metallic. In the absence of disorder within the tubes, the intertube electronic transfer, defined as the matrix element of the transverse coupling between two neighboring tubes, integrated over spatial coordinates, is negligible because of the longitudinal wave vector mismatch between tubes of different helicities [43]. The rope can then be considered as made of independent nanotubes in parallel. The transport is ballistic and the dimensionless conductance (in units of the quantum conductance $G_Q = 2e^2/h$) of the rope is two times the number of its metallic tubes. However, it has been shown [43,44] that disorder within the tubes favors intertube scattering by relaxing the strict orthogonality between the longitudinal components of the wave functions.

Using a very simple model in which disorder is treated perturbatively, we have shown [45] that the intertube scattering time can be shorter than the elastic scattering time within a single tube. In tubes longer than the elastic mean free path, this intertube scattering provides thus additional conducting paths to electrons which would otherwise be localised in isolated tubes. In the limit of localised transport along the tubes it is possible to show that the longitudinal localisation length of a rope is not a monotonous function of disorder and increases at moderate disorder. In order to go beyond these simple analytical results we have performed numerical simulations on a tight binding model of coupled 1D chains with different longitudinal hopping energies $t_{\|}$ [45]. This model mimics the physics of transport in a rope of carbon nanotubes in the sense that in the absence of disorder the electronic motion is localised within each chain. Transverse delocalisation as a function of disorder was investigated through the sensitivity of eigen-energies to a change of transverse boundary conditions from periodic to antiperiodic [46].

These results displayed in Fig. 4 show that disordered ropes of carbon nanotubes can be considered as anisotropic diffusive conductors, which, in contrast to individual tubes, exhibit a localisation length that can be much greater than the elastic mean free path. As a consequence, ropes of SWNT contacted using the laser nano-soldering technique present a much wider range of resistance values than individual tubes: the resistances vary between less than 100 Ω and 10^5 Ω at 300 K. There is also no systematic relation between the diameter of a rope and the value of its resistance. This may indicate that in certain cases only a small fraction of the tubes within a rope are well connected on both

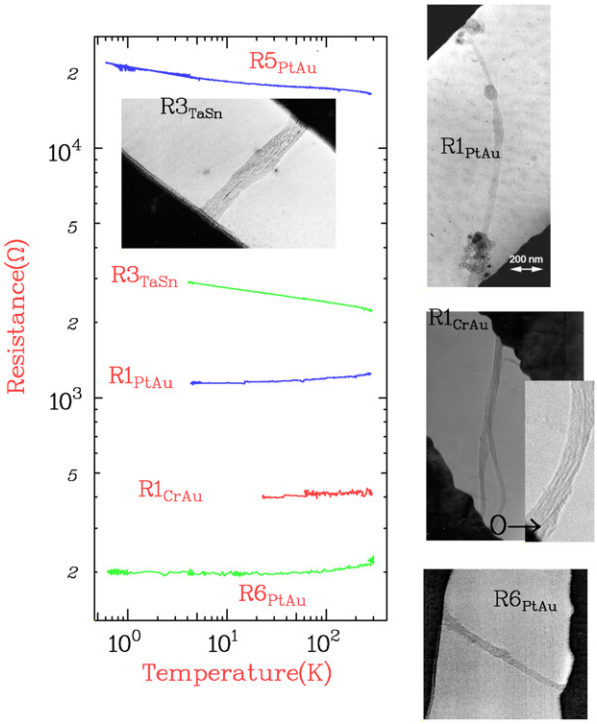

Fig. 5. Temperature dependence of the resistance measured on different ropes mounted on various types of contacts. For all samples the measurements were conducted in a magnetic field of 1 T. Note the logarithmic scales. The names of the samples refer to the metals that make up the electrodes. The diameters of the ropes vary between 20 to 30 nm which correspond to a number of tubes between 100 to 200.

contacts. In contrast to individual nanotubes, the ropes seem to verify the Thouless criterion [47]: they strongly localise when their resistance is above 10 kΩ at room temperature and stay quasi-metallic otherwise. This behavior is very similar to phase coherent quasi 1D metallic wires. The temperature dependence of low resistance ropes is found to be very weak (Fig. 5). But for low resistance ropes ($R < 10\,\mathrm{k}\Omega$) it is not monotonous, in contrast to individual tubes: the resistance decreases linearly as temperature decreases between room temperature and 30 K indicating the freezing-out of "twiston phonon modes" [48], and then increases as T is further decreased, as in individual tubes.

3.2. *Sub-Kelvin superconductivity in suspended ropes of SWNT on normal contacts*

In the following we discuss the low temperature transport (below 1 K) of suspended *ropes* of SWNT connected to normal electrodes. The electrodes are trilayers of sputtered Al_2O_3/Pt/Au of respective thicknesses 5, 3 and 200 nm.

As shown in Fig. 6, sample dependent behaviors are observed for the temperature dependence of the resistance measured in the linear response regime. The resistance of some samples ($R3_{PtAu}$ and $R6_{PtAu}$) increases weakly and monotonously as T is reduced, whereas the resistance of others ($R1, 2, 4, 5_{PtAu}$) drops over a relatively broad temperature range, starting below a temperature T^* between 0.4 and 0.1 K ($T_1^* = 140$ mK, $T_2^* = 550$ mK, $T_4^* = 100$ mK). The resistance of $R1_{PtAu}$ is reduced by 30% at 70 mK and that of $R4_{PtAu}$ by 75% at 20 mK. In both cases no inflection point in the temperature dependence is observed. On the other hand the resistance of $R2_{PtAu}$ decreases by more than two orders of magnitude, and reaches a constant value $R_r = 74\ \Omega$ below 100 mK. This drop of resistance disappears at a magnetic field above 1 T where the resistance increases with decreasing temperature, similarly to ropes 3 and 6, and becomes independent of magnetic field. These data suggest that the ropes 1, 2, 4 and 5 (first cool down) present intrinsic superconducting fluctuations.

In the temperature and field range where the zero-bias resistance drops, the differential resistance is strongly current-dependent, with lower resistance at low current; see Fig. 7. The differential resistance displays a large number of peaks whose density increases with the value of the current and the resistance of the sample. They can be attributed to the formation of small normal regions around defects (phase slip centers) when the current is increased [14]. The

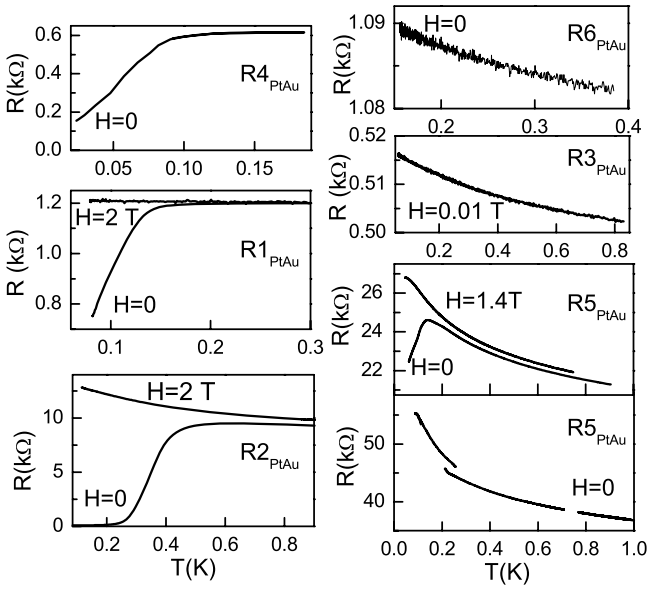

Fig. 6. Resistance as a function of temperature for various ropes of carbon nanotubes connected to non-superconducting electrodes. Note the absence of transition on the rope R5 after a thermal cycling which resulted in an increase of its resistance.

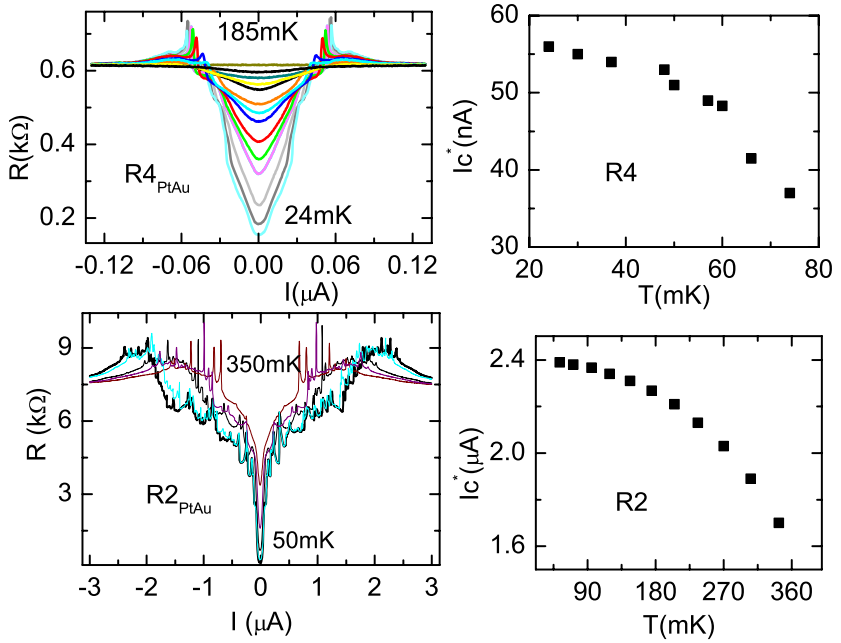

Fig. 7. Differential resistance of $R2_{PtAu}$ (disordered diffusive rope) and $R4_{PtAu}$ (ballistic rope), at different temperatures. Right panel: temperature dependence of I_c^*, the current at which the last resistance jumps occur in the dV/dI curves.

density of phase slips is found to be much higher in disordered ropes like $R2_{PtAu}$ compared to ballistic ones. Note also the major difference between this data and what is measured on SWNTs connected to superconducting contacts [13,14]: the $V(I)$, $dV/dI(I)$ curves do not show any supercurrent because of the existence of a finite residual resistance due to the contacts being normal.

Before analysing the data further we wish to emphasise that this is the first observation of intrinsic superconductivity in wires having less than one hundred conduction channels. Earlier experiments in nanowires [49–52] dealt with

at least a few thousand channels. We therefore expect a strong 1D behavior for the transition. In particular, due to large fluctuations of the superconducting order parameter in reduced dimension the resistance drop extends on a wide range of temperature starting at the 3D transition temperature T^* down to zero temperature. In the following we will attribute the variety of behaviors observed to several essential features: the large normal contacts, together with the finite length of the samples compared to relevant mesoscopic and superconducting scales, the number of tubes within a rope, the amount of disorder and intertube coupling, and finally the suspended character of the tubes. We first assume that all ropes are diffusive conductors but we will see that this hypothesis is probably not valid in the most ordered ropes.

3.2.1. Normal contacts and residual resistance

We first recall that the conductance of any superconducting wire measured through normal contacts is limited by N_c/R_Q where N_c is the number of conducting channels of the superconductor in contact with the normal reservoir. A metallic SWNT, with 2 conducting channels, has a contact resistance of half the resistance quantum, $R_Q/2$ even if it is superconducting. A rope of N_m parallel metallic SWNT will have a minimum resistance of $R_Q/(2N_m)$ in the S state. Therefore we use the residual resistance R_r measured at the lowest temperature, to deduce a lower bound for the number of metallic tubes in the rope $N_m = R_Q/2R_r$. From the residual resistances of 74 Ω in sample $R2_{PtAu}$, and less than 170 Ω in $R4_{PtAu}$ we deduce that there are at least ≈ 90 metallic tubes in $R2_{PtAu}$ (which contains 300 tubes) and ≈ 40 in $R4_{PtAu}$ (which contains 50 tubes). In both cases that means that a large fraction of tubes take part in the conduction and justifies a posteriori the hypothesis that ropes are multichannel possibly diffusive conductors.

3.2.2. Destruction of superconductivity by the normal contacts

What are the parameters characterising the superconductivity in the ropes? Assuming that the BCS relation holds we get for the superconducting gap $\Delta = 1.76\, k_B T^*$: $\Delta \approx 85$ μeV for $R2_{PtAu}$. We can then deduce the superconducting coherence length along the rope in the diffusive limit:

$$\xi = \sqrt{\hbar v_F l_e/\Delta} \tag{1}$$

where l_e is the elastic mean free path which characterises the amplitude of disorder and can be deduced from the high temperature value of the resistance of the rope and the number of contacted metallic tubes. This expression yields $\xi_2 \approx 0.3$ μm where v_F is the longitudinal Fermi velocity 8×10^5 m/s. We now estimate the superconducting coherence length of the other samples, to explain the extent or absence of observed transition. Indeed, investigation of the proximity effect at high-transparency NS interfaces has shown that superconductivity resists the presence of normal contacts only if the length of the superconductor is much greater than ξ [53]. This condition is nearly fulfilled in $R2_{PtAu}$ ($\xi_2 \approx L_2/3$). Taking the same value of Δ for all samples, we find $\xi_1 \approx L_1/2$, $\xi_4 \approx L_4/2$, $\xi_3 \approx 2L_3$, and $\xi_6 \approx 2L_6$. These values explain qualitatively the reduced transition temperature of $R1_{PtAu}$ and $R4_{PtAu}$ and the absence of a transition for $R3_{PtAu}$ and $R6_{PtAu}$ see Fig. 6. It is, however, not possible to explain the behavior of the sample 5 with the same kind of argument, since the same expression yields a coherence length ξ_5 much shorter than the length of the sample, and nonetheless no complete transition is seen. We believe that this is due to the strong disorder in this sample which is very close to the localisation limit. These results emphasise also the particular role of disorder which on one hand favors superconductivity by reducing l_e and accordingly the ratio ξ/L but on the other hand leads to localisation if it is too important.

3.2.3. Role of the number of tubes

Another a priori important parameter is the number of tubes in a rope: the less tubes in a rope, the closer the system is to the strictly 1D limit, and the weaker the transition. If we compare the ropes $R2_{PtAu}$ and $R4_{PtAu}$ in Fig. 6, it is clear that the transition both in temperature and magnetic field is much broader in the rope $R4_{PtAu}$ with only 40 tubes than in the rope $R2_{PtAu}$ with 350 tubes. Moreover there is no inflexion point in the temperature dependence of the resistance in the thinner rope, typical of a strictly 1D behavior. We also expect a stronger screening of e–e interactions in a thick rope compared to a thin one, which could also favor superconductivity as we will discuss below.

3.2.4. Role of disorder and intertube coupling

As is clear from expression (1) for the superconducting coherence length, disorder is at the origin of a reduction of the superconducting coherence length in a diffusive sample compared to a ballistic one and can in this way also

decrease the destructive influence of the normal contacts. More subtle and specific to the physics of ropes, we have seen that disorder also enhances the intertube coupling, so it can increase the dimensionality of the superconducting transition: weakly disordered ropes like R1 and R4 will be more 1D-like than the more disordered rope R2. Of course disorder must always be sufficiently small so as not to induce localisation. These considerations may explain the variety of behaviors observed and depicted in Fig. 6.

Finally, disorder is also the essential ingredient which reveals the difference between the normal state and the superconducting state. In a ballistic rope we would not expect to observe a variation of the resistance over the superconducting transition because in both cases the resistance of the rope is just the contact resistance.

To gain insight in the transport regime, we have performed shot noise measurements of the ropes $R1, 3, 4, 6_{PtAu}$, in the normal state (higher level of 1/f noise in the more resistive ropes $R2, 5_{PtAu}$ made the analysis of shot noise impossible in those samples), between 1 and 15 K. The shot noise power of these low resistive ropes in the normal state was found to be of the order of $S_I = 2eI/100$, much less than the shot noise power $S_I = 2eI/3$ expected for a coherent diffusive sample. Such a large reduction could be the signature of ballistic transport through the rope [54] and implies that all the tubes in these ropes are either completely ballistic or completely localised [54]. This is in apparent contradiction with the observation of the superconducting transition of $R4_{PtAu}$, with a 60% resistance drop.

It is, however, possible to explain a resistance decrease in ballistic ropes turning superconducting, if the number of conducting channels is larger for Cooper pairs than for individual electrons. In his theoretical investigation of superconductivity in ropes of SWNT, Gonzalez [55] has shown the existence of a finite intertube transfer for Cooper pairs, even between two tubes of different helicities which have no possibility of single electron intertube transfer. This Cooper pair delocalisation could lead to the opening of new channels when a rope, containing a mixture of insulating and ballistic tubes not all connected to the electrodes, becomes superconducting.

3.2.5. Suspended character of the tubes

In order to investigate the importance the suspended character of the SWNT ropes, we have gradually coated a suspended rope of SWNT with organic materials. We observed that superconductivity was gradually destroyed. Parallel Raman experiments on other samples showed that the radial breathing modes are affected by coating, thereby hinting to these modes as playing a major role in the superconductivity of carbon nanotubes.

The sample whose superconductivity we have altered is a rope containing roughly 40 SWNT (sample $R4_{PtAu}$). The number of conducting SWNTs is determined from the normal state resistance, given that the two wire resistance of a SWNT is at least $h/4e^2 \approx 6.5$ kΩ. In the normal state, transport proceeds via ten ballistic tubes. It is likely that the 10 tubes through which current flows in the normal state are those at the circumference of the rope. But in the superconducting state, Cooper pairs can delocalise over all the superconducting tubes since their total momentum is zero [55].

The sample was then modified in successive steps. We first (stage *b*) coated it at room temperature with a drop of benzenedithiol. In step *c*, we coated the rope with polymethyl methacrylate (PMMA) which is more viscous than benzenedithiol. In step *d* more PMMA was added, so that the entire slit was covered with PMMA. The trend upon successive coatings, presented in Fig. 8, is to have a slightly modified normal state (high temperature) resistance, which varies between 550 and 750 Ω, and more spectacularly a superconducting transition which weakens as the nanotube rope is coated. The transition temperature T^*, defined as the temperature at which the resistance starts to decrease, which would be the transition temperature of a (hypothetical) corresponding 3D superconductor, shifts from 120 mK to 60 mK in curves *a* to *c*. In curve *d*, the coating is so important that no transition is visible down to less than 15 mK. The resistance even increases by 0.5% between 200 mK and 16 mK.

The gradual weakening of the rope's superconductivity is also clearly seen in the differential resistance curves with a disappearance of any detectable low bias anomaly in the coated rope.

To understand the link between the weakening of superconductivity and the effect of coating on the phonon modes of these ropes, we have investigated the effect of PMMA deposition on the Raman response of other suspended nanotubes [56]. We compared the *relative* intensity of the RBM with respect to the tangential modes (TM). In the uncoated sample, the intensity of the RBM peak at 200 cm^{-1} is much greater than the intensity of the TM at 1600 cm^{-1}. This is due to the fact that the tubes are suspended, and therefore do not interact through Van der Waals interaction with the substrate [57]. With coating we find that the RBM intensity becomes much smaller (at least an order of magnitude) than the intensity of the TM. After removal of the PMMA with acetone, the overall Raman intensity is recovered, as is the large intensity of the metallic RBM relative to the TM.

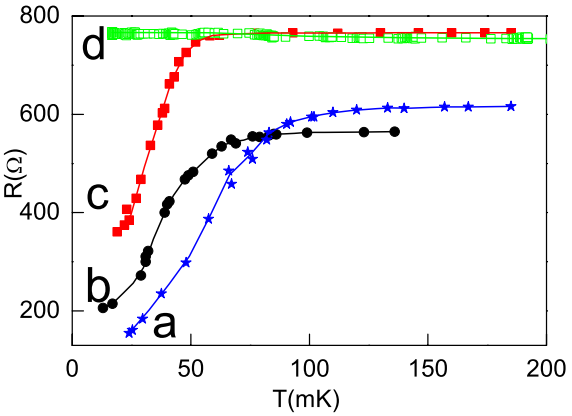

Fig. 8. Temperature dependence of the resistance of the 10 nm wide, 1 μm-long rope containing 40 SWNT. (a) Before coating. (b) After benzene–dithiol deposition. (c) After additional coating with PMMA. (d) After completely covering the rope and the slit with PMMA. Lines are guides to the eyes.

The fact that the absolute RBM signal is much larger for suspended tubes than for tubes on a substrate has also been observed in recent Scanning Tunneling Microscopy experiments on suspended nanotubes [58]. The authors found the spectroscopic signature of the RBM modes only on the suspended portions of the tubes, and not on the contact regions. But our experiment also shows that coating tubes with PMMA suppresses their RBM *much more* than the TM. In the transport experiment on the rope containing 40 tubes, it is therefore likely that the RBM of the tubes on the surface of the rope are suppressed because they are coated by PMMA. The disappearance of superconductivity could therefore be explained by the fact that the blocking of the RBM of the 10 connected outer tubes causes the suppression of their superconducting transition. Although the inner tubes which are uncoated by PMMA could still be superconducting, the superconducting transition would not be seen in a transport experiment since there is barely any electronic transfer between normal external tubes and inner tubes in a rope with little disorder [55].

We have thus shown that coating nanotubes with polymers suppresses the radial breathing modes of individual SWNTs, and suppresses the superconducting transition of a suspended rope of 40 SWNTs. This suggests that the RBM could be the phonon responsible for the phonon mediated attractive interaction responsible for the superconductivity of carbon nanotubes.

3.3. Meissner effect in ropes of carbon nanotubes

Beside transport, it is also essential to investigate thermodynamic signatures such as the Meissner effect of this unusual superconductivity. The geometry of carbon nanotubes, which are very narrow 1D cylinders, is a priori not favorable for efficient magnetic flux expulsion. Nevertheless, magnetisation measurements performed on very small (0.4 nm) diameter SWNT, revealed a diamagnetic contribution increasing at low temperature below 6 K [60] which was interpreted as superconducting fluctuations. However the geometry of the samples grown in zeolite matrices was not adequate for transport measurements, which did not show clear sign of superconductivity.

We have also addressed this question of flux expulsion (i.e. the Meissner effect) by measuring the magnetisation of ropes of SWNT similar to those previously studied in transport measurements [61]. The magnetic signal contains unfortunately an important contribution coming from residual catalyst iron particles in the purified ropes of carbon nanotubes. They mostly give rise to a hysteretic contribution which does not change with temperature below 35 K. At low temperature, it was thus possible to decompose the magnetic signal into a T independent contribution attributed to frozen large magnetic particles and into a temperature dependent part which is reversible. We have shown [61] that beside this contribution of unfrozen superparamagnetic particles, it is possible to identify the presence of a diamagnetic low field dependent contribution growing below 0.4 K which provides a strong indication of the existence of a Meissner contribution in ropes of SWNT, in agreement with the onset of superconductivity observed in transport measurements realised on similar samples; see Fig. 9. From the partial alignment of the tubes in the samples, it was also possible to probe the anisotropy of the Meissner effect.

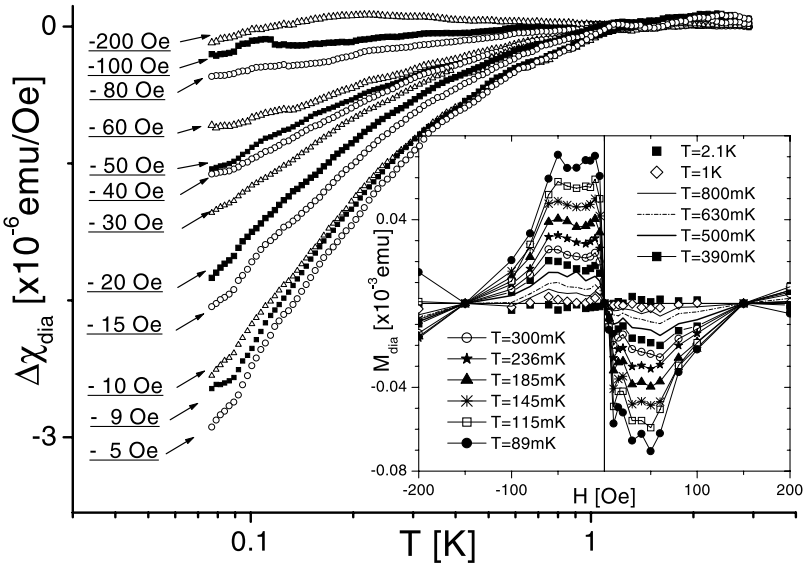

Fig. 9. Temperature dependence of the magnetisation of an assembly of ropes of carbon nanotubes after subtraction of the superparamagnetic contribution of the catalyst particles. Insert: Reconstitution of the field dependence of the diamagnetic contribution for various temperatures. Note the small values of critical field (related to the breaking of Josephson coupling between the tubes within a rope) compared to the much larger value in the Tesla range observed in transport experiments.

4. Conclusion and perspectives

Data depicted in the previous section show the existence of intrinsic superconductivity in ropes of carbon nanotubes comprising between 40 and 400 nanotubes. The question of the existence of superconducting correlations in the limit of the individual tube cannot be answered yet. It is, of course, tempting to consider the high supercurrent measured on superconducting contacts as a strong indication that superconducting fluctuations are present also in individual carbon nanotubes. However, since unscreened Coulomb repulsive interactions in these samples are expected to suppress superconductivity, precise investigations of individual carbon nanotubes on normal contacts are necessary. It is essential to conduct experiments on sufficiently long samples (such as the ropes presently studied) so that intrinsic superconductivity is not destroyed by the normal contacts. The experiments conducted down to low temperature to this day outline the stringent requirements to observe superconductivity: nanotubes should not be coated by polymers, and should be suspended. They should be long enough in order to avoid the inverse proximity effect, which causes the proximity to normal contacts to destroy the superconductivity in the tubes. Finally, there should be efficient screening of the repulsive interaction in nanotubes, so that superconductivity should develop most in tubes that are assembled in a rope.

4.1. What is the mechanism of superconductivity in carbon nanotubes?

We now discuss what could be the relevant mechanism for superconductivity in carbon nanotubes. Observation of superconductivity in carbon based compounds was reported a long time ago. First in graphite intercalated with alkali atoms (Cs, K), superconducting transitions were observed between 0.2 and 0.5 K [64]. Much higher temperatures were observed in alkali-doped fullerenes [65]. In all these experiments it was essential to chemically dope the system to observe superconductivity. There is no such chemical dopants in the ropes of carbon nanotubes discussed above but there is some possibility of hole doping of the tubes by the gold metallic contacts which electronic work function is larger than that of the tubes [66,67]. However, although this doping could slightly depopulate the highest occupied energy band in a semiconducting tube it is very unlikely that it is strong enough to depopulate other lower energy subbands for a metallic tube with a diameter in the nm range. We will see on the other hand that intentionally doped carbon nanotubes exhibit superconducting fluctuations at much higher temperature than what we have observed.

As for doped fullerene molecules [2], the question of which phonons give rise to the attractive interaction leading to superconductivity is still unsettled. Whereas Sédéki et al. [69] and Gonzalez [55] consider the coupling to optical phonons, De Martino and Egger [59] conjecture that attractive interactions can be mediated by low energy phonon modes specific to the structure of carbon nanotubes, in particular the radial breathing modes (RBM), which is compatible with our experimental results depicted above. They find that the attractive interaction may be strong enough to overcome the repulsive interactions in SWNT, especially in ropes of SWNT where the Coulomb interaction can be screened because the SWNT are packed so closely together. Their theory [59] also could reproduce the temperature dependence of the superconducting transition observed in ropes as well as its dependence on the number of tubes [63]. A purely electronic coupling mechanism has also been shown to induce superconducting fluctuations in carbon nanotubes expected to behave like coupled double chain systems such as ladders [68]. The very small order of magnitude for the energy scale of these superconducting fluctuations does not seem however to be compatible with experimental findings [59,62,67].

4.2. Signatures of superconductivity at "high" temperature

Other experiments have also shown evidence of intrinsic superconductivity in carbon nanotubes at temperatures as high as 10 K. This was first the case in magnetisation experiments [60] which strongly supported the existence of anisotropic superconducting fluctuations below 6 K in very small diameter (0.4 nm) individual tubes grown in zeolites. This high value of T_c was explained by the very small diameter of the tubes leading to a breathing mode at much higher energies compared to the 1.2 nm diameter nanotubes we have investigated. More recently resistance measurements performed on arrays of multiwall carbon nanotubes (MWNT) have been shown to exhibit a sharp drop of resistances around 12 K. These results have, however, been found to strongly depend on the way the nanotubes were connected, indicating that only small diameter internal shells were exhibiting superconductivity [70]. It was then shown that these samples were doped with boron and that this doping was playing an essential role in stabilising the superconductivity. This was recently confirmed by magnetisation experiments on intentionally boron doped arrays of SWNT constituting thin films. For boron concentrations between 1 and 3 at.% the low field dependent magnetisation is compatible with a Meissner effect at temperatures below 12 K and magnetic field below 0.4 T [71]. Finally, even more surprising, superconducting fluctuations (resistance drop below 20 K) have been observed in individual gated SWNT [72] in good contacts with normal electrodes. These fluctuations were found only for fairly high values of gate voltages indicating the importance of carrier doping also in these experiments. It is suggested (like in previous experiments), that it may be possible to enter a regime where the Fermi energy is aligned with a van Hove singularity characteristic of the band structure of a SWNT.

References

[1] P.R. Wallace, Phys. Rev. 71 (1947) 622.
[2] M.S. Dresselhaus, G. Dresselhaus, P.C. Eklund, Science of Fullerenes and Carbon Nanotubes, Academic, San Diego, 1996.
[3] J.C. Charlier, X. Blase, S. Roche, Rev. Mod. Phys. 79 (2007) 677.
[4] R. Egger, A. Gogolin, Phys. Rev. Lett. 79 (1997) 5082;
R. Egger, Phys. Rev. Lett. 83 (1999) 5547.
[5] C. Kane, L. Balents, M.P. Fisher, Phys. Rev. Lett. 79 (1997) 5086.
[6] M. Bockrath, D.H. Cobden, J. Lu, A.G. Rinzler, R.E. Smalley, L. Balents, P.L. McEuen, Nature 397 (1999) 598.
[7] H. Grabert, M.H. Devoret (Eds.), Single Charge Tunneling, Plenum, New York, 1992;
S.J. Tans, M.H. Devoret, H.J. Dai, A. Thess, R.E. Smalley, L.J. Geerligs, C. Dekker, Nature 386 (1997) 474.
[8] A.Yu. Kasumov, I.I. Khodos, P.M. Ajayan, C. Colliex, Europhys. Lett. 34 (1996) 429;
A.Yu. Kasumov, et al., Europhys. Lett. 43 (1998) 89.
[9] J. Nygard, D.H. Cobden, P.E. Lindelof, Nature 408 (2000) 342.
[10] W. Liang, M. Bockrath, D. Bozovic, J.H. Hafner, M. Tinkham, H. Park, Nature 411 (2001) 665.
[11] I. Safi, H.J. Schulz, Phys. Rev. B 52 (1995) R17040.
[12] D. Goldhaber-Gordon, H. Shtrikman, D. Mahalu, D. Abusch-Magder, U. Meirav, M.A. Kastner, Nature 391 (1998) 156.
[13] A.Yu. Kasumov, R. Deblock, M. Kociak, B. Reulet, H. Bouchiat, I.I. Khodos, Yu.B. Gorbatov, V.T. Volkov, C. Journet, M. Burghard, Science 284 (1999) 1508.
[14] A. Kasumov, M. Kociak, M. Ferrier, R. Deblock, S. Guéron, B. Reulet, I. Khodos, O. Stéphan, H. Bouchiat, Phys. Rev. B 68 (2003) 214521.
[15] H. Courtois, Ph. Gandit, B. Panetier, Phys. Rev. B 52 (1995) 1162.
[16] P. Dubos, H. Courtois, B. Pannetier, F.K. Wilhelm, A.D. Zaikin, G. Schön, Phys. Rev. B 63 (2001) 064502.

[17] L. Angers, F. Chiodi, G. Montambaux, M. Ferrier, S. Guéron, H. Bouchiat, J.C. Cuevas, Phys. Rev. B 77 (2008) 165408.
[18] For reviews of supercurrents through superconducting junctions see: K. Likharev, Rev. Mod. Phys. 51 (1979) 101;
A.A. Golubov, M.Yu. Kupriyanov, E. Il'ichev, Rev. Mod. Phys. 76 (2004) 411.
[19] R. Fazio, F.W.J. Hekking, A.A. Odintsov, Phys. Rev. B 53 (1995) 6653.
[20] D. Maslov, M. Stone, P.M. Goldbart, D. Loss, Phys. Rev. B 53 (1995) 1548.
[21] I. Affleck, J.B. Caux, A. Zagoskin, Phys. Rev. B 62 (2000) 1433.
[22] J. Gonzalez, Phys. Rev. Lett. 87 (2001) 136401.
[23] P. Poncharal, Z.L. Wang, D. Ugarte, W.A. de Heer, Science 283 (1999) 1513.
[24] J.W. Wildoer, et al., Nature 391 (1998) 59.
[25] B. Reulet, A.Yu. Kasumov, M. Kociak, R. Deblock, I.I. Khodos, Yu.B. Gorbatov, V.T. Volkov, C. Journet, H. Bouchiat, Phys. Rev. Lett. 85 (2000) 2829.
[26] V. Sazonova, Y. Yaish, H. Ustunel, D. Roundy, T.A. Arias, P.L. McEuen, Nature 431 (2004) 284;
D. Garcia-Sanchez, A. San Paulo, M.J. Esplandiu, F. Perez-Murano, L. Forró, A. Aguasca, A. Bachtold, Phys. Rev. Lett. 99 (2007) 085501.
[27] A. Zazunov, D. Feinberg, T. Martin, Phys. Rev. Lett. 97 (2006) 196801.
[28] A.F. Morpurgo, J. Kong, C.M. Marcus, H. Dai, Science 286 (1999) 263.
[29] M.R. Buitelaar, T. Nüssbaumer, C. Schönenberger, Phys. Rev. Lett. 89 (2002) 256801;
M.R. Buitelaar, W. Belzig, T. Nussbaumer, B. Babic, C. Bruder, C. Schönenberger, Phys. Rev. Lett. 91 (2003) 057005.
[30] I. Jorgensen, K. Grove-Rasmussen, T. Novotny, K. Flensberg, P.E. Lindelof, Phys. Rev. Lett. 96 (2006) 207003.
[31] P. Jarillo-Herrero, J.A. van Dam, L.P. Kouwenhoven, Nature 439 (2006) 953;
More recently, tunable supercurrents through Carbon nanotubes have also been observed in T. Tsuneta, L. Lechner, P. Hakonen, Phys. Rev. Lett. 98 (2007) 087002;
Y. Zhang, G. Liu, C.N. Lau, Nano Res. 1 (2008) 145;
E. Pallecchi, M. Gaaß, D.A. Ryndyk, C. Strunk, Appl. Phys. Lett. 93 (2008) 072501;
G. Liu, Y. Zhang, C.N. Lau, cond-mat/0806.2642.
[32] J.-P. Cleuziou, W. Wernsdorfer, V. Bouchiat, T. Ondarcuhu, M. Monthioux, Nat. Nanotechnol. 1 (2006) 53;
Note that similar devices were made with semiconducting nanowire: J.A. van Dam, Y.V. Nazarov, E.P.A.M. Bakkers, S. De Franceschi, L.P. Kouwenhoven, Nature 442 (2006) 667.
[33] I. Jorgensen, T. Novotny, K. Grove-Rasmussen, K. Flensberg, P.E. Lindelof, Nano Lett. 7 (2007) 2441.
[34] L.I. Glazman, K.A. Matveev, JETP Lett. 49 (1989) 659.
[35] A.V. Rozhkov, D.P. Arovas, Phys. Rev. Lett. 82 (1999) 2788.
[36] M.-S. Choi, M. Lee, K. Kang, W. Belzig, Phys. Rev. B 70 (2004) 020502.
[37] E. Vecino, A. Martin-Rodero, A. Levy Yeyati, Phys. Rev. B 68 (2003) 035105.
[38] F. Siano, R. Egger, Phys. Rev. Lett. 94 (2005) 229702.
[39] C. Karrasch, A. Oguri, V. Meden, Phys. Rev. B 77 (2008) 024517.
[40] K. Grove-Rasmussen, H.I. Jorgensen, P.E. Lindelof, New J. Phys. 9 (2007) 124.
[41] A. Eichler, et al., Phys. Rev. B 79 (2009) 161407.
[42] C. Journet, W. Maser, P. Bernier, A. Loiseau, M.L. de la Chapelle, S. Lefrant, P. Deniard, R. Lee, J. Fisher, Nature 388 (1997) 756.
[43] A. Maarouf, C. Kane, E. Mele, Phys. Rev. B 61 (16) (2000) 11156.
[44] M.A. Tunney, N.R. Cooper, Phys. Rev. B 74 (16) (2006) 075406.
[45] M. Ferrier, A. Chepelianskii, S. Guéron, H. Bouchiat, Phys. Rev. B 77 (2008) 195420.
[46] J.T. Edwards, D.J. Thouless, J. Phys. C: Solid State Phys. 5 (1972) 807.
[47] D.J. Thouless, Phys. Rev. Lett. 39 (1977) 1967.
[48] C.L. Kane, et al., Europhys. Lett. 41 (1998) 683.
[49] N. Giordano, Phys. Rev. B 50 (1991) 160.
[50] F. Sharifi, A.V. Herzog, R.C. Dynes, Phys. Rev. Lett. 71 (1993) 428–431;
P. Xiong, A.V. Herzog, R.C. Dynes, Phys. Rev. Lett. 78 (1997) 927–930.
[51] C.N. Lau, N. Markovic, M. Bockrath, A. Bezryadin, M. Tinkham, Phys. Rev. Lett. 87 (2001) 217003;
M. Zgirski, et al., Nano Lett. 5 (2005) 1029;
M. Zgirski, K.-P. Riikonen, V. Touboltsev, K.Yu. Arutyunov, Phys. Rev. B 77 (2008) 054508.
[52] F. Lucot, F. Pierre, D. Mailly, K. Yu-Zhang, S. Michotte, F. De Menten de Horne, L. Piraux, Appl. Phys. Lett. 91 (2007) 042502.
[53] W. Belzig, C. Bruder, G. Schön, Phys. Rev. B 54 (1996) 9443.
[54] P. Roche, M. Kociak, S. Guéron, A. Kasumov, B. Reulet, H. Bouchiat, Eur. Phys. J. B 28 (2002) 217–222.
[55] J. Gonzalez, Phys. Rev. Lett. 87 (2001) 136401;
J. Gonzalez, Phys. Rev. Lett. 88 (2002) 076403;
J. Gonzalez, Phys. Rev. B 67 (2003) 014528.
[56] M. Ferrier, A.Yu. Kasumov, V. Agache, L. Buchaillot, A.-M. Bonnot, C. Naud, V. Bouchiat, R. Deblock, M. Kociak, M. Kobylko, S. Guéron, H. Bouchiat, Phys. Rev. B 74 (2006) 241402.
[57] L. Marty, Ph.D. thesis, Université J. Fourier, Grenoble I, 2004.
[58] B.J. LeRoey, S.G. Lemay, J. Kong, C. Dekker, Nature 371 (2005) 432;
B.J. LeRoey, S.G. Lemay, J. Kong, C. Dekker, Appl. Phys. Lett. 84 (2004) 4280.
[59] A. De Martino, R. Egger, Phys. Rev. B 67 (2003) 235418;
A. De Martino, R. Egger, Phys. Rev. B 70 (2004) 014508.

[60] Z. Tang, L. Zhang, N. Wang, X. Zhang, G. Wen, G. Li, J. Wang, C. Chan, P. Sheng, Science 292 (2001) 2462–2465.
[61] M. Ferrier, F. Ladieu, M. Ocio, B. Sacépé, T. Vaugien, V. Pichot, P. Launois, H. Bouchiat, Phys. Rev. B 73 (2006) 094520.
[62] M. Ferrier, et al., Solid State Commun. 131 (9–10) (2004) 615.
[63] M. Ferrier, A. de Martino, A. Kasumov, S. Guéron, M. Kociak, R. Egger, H. Bouchiat, Solid State Commun. 131 (2004) 615.
[64] N.B. Hannay, T.H. Geballe, B.T. Matthias, K. Andres, P. Schmidt, D. MacNair, Phys. Rev. Lett. 14 (1965) 225.
[65] O. Gunnarsson, Rev. Mod. Phys. 69 (1997) 575.
[66] L.C. Venema, J.W.G. Wildöer, J.W. Janssen, S.J. Tans, H.L.J. Temminck Tuinstra, L.P. Kouwenhoven, C. Dekker, Science 283 (1999) 52.
[67] A.A. Odintsov, Phys. Rev. Lett. 85 (2000) 150.
[68] H.J. Schulz, Phys. Rev. B 53 (1996) R2959.
[69] A. Sédéki, L.G. Caron, C. Bourbonnais, Phys. Rev. B 65 (2002) 140515.
[70] I. Takesue, et al., Phys. Rev. Lett. 96 (2006) 057001.
[71] N. Murata, J. Haruyama, J. Reppert, A.M. Rao, T. Koretsune, S. Saito, M. Matsudaira, Y. Yagi, Phys. Rev. Lett. 101 (2008) 027002.
[72] J. Zhang, A. Tselev, Y. Yang, K. Hatton, P. Barbara, S. Shafraniuk, Phys. Rev. B 74 (2006) 155414.